MATERIALS CHEMISTRY
FRONTIERS

RESEARCH ARTICLE

View Article Online
View Journal | View Issue

Cite this: *Mater. Chem. Front.*, 2019, **3**, 2751

Microwave-assisted synthesis of nitrogen-rich carbon dots as effective fluorescent probes for sensitive detection of Ag^+†

Jie Feng,[a] Xiaoran Zhao,[a] Wei Bian[b] and Xinjing Tang *[a]

Received 9th October 2019,
Accepted 23rd October 2019

DOI: 10.1039/c9qm00624a

rsc.li/frontiers-materials

A simple strategy for the synthesis of fluorescent nitrogen-rich carbon dots (N-dots) is developed through microwave-assisted reaction of 2-azidoimidazole with different hydroxyl compounds. With the increase of hydroxyl groups of the crosslinkers, the emission property of the corresponding N-dots was enhanced. Among them, N-dots with 2-azidoimidazole and glycerol as the starting materials showed high monodispersity, good stability, excellent water solubility and strong fluorescence emission with fluorescence quantum yield up to 27.9%. These N-dots were further employed as an effective chemosensor for Ag^+ analysis *via* the static quenching effect and a good linear range of Ag^+ detection was obtained from 20 nM to 6 μM with a limit of detection of 6.3 nM, displaying high selectivity toward Ag^+ detection in real samples.

Introduction

In previous decades, fluorescent carbon dots (CDs) have attracted tremendous attention due to their unique properties, including strong fluorescence, good biocompatibility, excellent solubility, and easy surface modification. These characteristics make CDs new nanocarriers in various applications, such as bioimaging,[1] sensing,[2,3] catalysis,[4,5] photoelectronics,[6,7] and energy conversion/storage devices.[8] So far, many different methods have been developed to fabricate CDs. Kang *et al.* synthesized biomolecule-mimicking nitrogen-doped CDs from dopamine by a neutralization heating strategy.[9] Wang *et al.* established a plasma-induced method for the preparation of stable CDs with natural chicken eggs as the precursor and used these CDs as fluorescent inks.[10] Multicolor fluorescent CDs with red, green, and blue emissions were prepared using three different phenylenediamine isomers *via* a solvothermal method.[11] Heteroatom doping was another one of the most effective routes to prepare CDs. Zuo *et al.* chose an aromatic fluorine source to synthesize a series of fluorine (F)-doped CDs by a solvothermal process. The prepared F-doped CDs were used for red cell imaging, sensing and gene delivery.[12,13] Recently, our group reported a new kind of nitrogen-rich quantum dot (N-dots) by heating 2-azidoimidazole methanol solution under mild conditions and applied them in biocompatible staining and sensing.[14,15] However, there were still some issues to be solved for CDs, such as uniform size, product yield and fluorescence quantum yield (QY). Accordingly, it is highly desirable to develop facile methods for the preparation of CDs. As previously reported, microwave heating is a fascinating and promising tool for the preparation of carbon materials.[16–18] Due to the rapid and direct heating, microwave heating enables the acceleration of reaction processes, which results in time- and energy-saving.[19] Moreover, the possibility of obtaining temperatures above the boiling point at increased pressure can result in the fast preparation of monodisperse, small-sized and highly pure nanoparticles.[19] Based on these advantages, the microwave-assisted methods have been rapidly developed for the preparation of CDs.[20,21]

In the present work, we reported a facile route to synthesize nitrogen-rich CDs (N-dots) using microwave heating treatment of 2-azidoimidazole and different hydroxyl compounds (propanol, 1,2-propanediol, and glycerol). By optimizing the experiment conditions, the as-synthesized N-dots using 2-azidoimidazole and glycerol as starting materials showed the highest fluorescence emission with fluorescence QY up to 27.9%. Along with strong fluorescence performance, these N-dots exhibited a homogeneous size distribution, good water solubility, and excellent stability. Further application as a "turn-off" fluorescent nanoprobe for sensitive and selective Ag^+ ion detection was achieved based on the static quenching mechanism (Scheme 1).

Results and discussion

Synthesis of nitrogen-rich CDs (N-dots)

In the present work, we first investigated the preparation of N-dots from 2-azidoimidazole aqueous solution without the

[a] *State Key Laboratory of Natural and Biomimetic Drugs, Department of Medicinal Chemistry, the School of Pharmaceutical Sciences, Peking University, Beijing 100191, China. E-mail: xinjingt@bjmu.edu.cn*
[b] *School of Basic Medical Science, Shanxi Medical University, Taiyuan 030001, China*

† Electronic supplementary information (ESI) available. See DOI: 10.1039/c9qm00624a

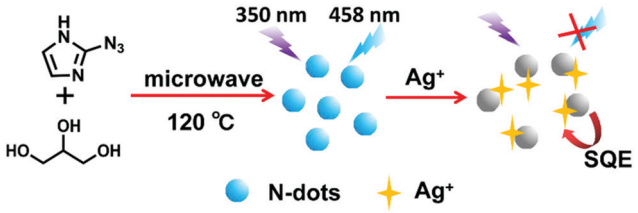

Scheme 1 Illustration of the synthesis process of nitrogen-rich CDs (N-dots) and the detection of Ag^+.

addition of alcohol under microwave-assisted heating. The obtained yellow-brown solution exhibited blue fluorescence with fluorescence quantum yield (QY) of 8.7% (Table S1, ESI†). As previously reported, weak fluorescent subfluorophores can generally enhance their fluorescence emission with suitable immobilization, such as covalent/supramolecular cross-linking or even physical aggregation.[22,23] To improve the QY of the above N-dots, we hypothesized that an appropriate additive was essential to construct a more cross-linked rigid core structure of carbon dots. According to the mechanism of our previous N-dot formation using 2-azidoimidazole methanol solution, the hydroxyl group of methanol involved the opening of aziridine in linear polymerization and N-dot formation.[14] Thus, in the present work, three hydroxyl compounds including propanol, 1,2-propanediol, and glycerol with the same three carbon atoms but different possible cross-linking degrees were employed as supramolecular crosslinking additives to synthesize fluorescent N-dots under the same conditions. Firstly, we confirmed that sole hydroxyl compounds (including propanol, 1,2-propanediol, and glycerol) themselves could not produce fluorescent N-dots under the same microwave heating conditions. With the addition of hydroxyl compounds to the 2-azidoimidazole aqueous solution, fluorescent N-dots were obtained. As expected, the QY of the prepared N-dots increased greatly from 10.9%, to 22.2% to 27.9% with the increase of hydroxyl groups from propanol, to 1,2-propanediol, and glycerol, respectively (Table S1, ESI†), which may be due to the increase of cross-linking possibility between the polymers formed from 2-azidoimidazole. As shown in Fig. S1 (ESI†), all N-dots synthesized from these hydroxyl compounds and 2-azidoimidazole exhibited similar absorption and fluorescence emission wavelength. These results indicated that all these N-dots contained the same emission fluorophore. At the same time, elemental analysis showed that the percentages of nitrogen element in these N-dots were 26.5%, 23.8%, and 35.3%, respectively, confirming the high percentage of nitrogen element.

In the following study, 2-azidoimidazole and glycerol with three hydroxyl groups were chosen as starting materials for the preparation of N-dots. To achieve the maximum fluorescence QY of N-dots, different reaction conditions (*e.g.* the concentration of glycerol, microwave heating time and temperature) were investigated. As shown in Fig. S2 (ESI†), the concentration of glycerol had a large effect on fluorescence properties. The QY of prepared N-dots reached the maximum value when the concentration of glycerol was around 50% (v/v) (glycerol/water) (Table S2, ESI†). Meanwhile, low reaction temperature greatly decreased the QY of N-dots when the reaction temperature was <100 °C, and microwave heating temperature between 100 °C and 140 °C was optimal (Fig. S3 and Table S3, ESI†). Thus, the optimal microwave reaction temperature was set to be 120 °C for further optimization. Microwave heating reaction time also played an important role in determining the fluorescence emission of N-dots. It was found that these N-dots with the highest QY were obtained within 30 min microwave heating (Fig. S4 and Table S4, ESI†). And the prolonged microwave heating led to the decrease of fluorescence emission of these N-dots, which was caused by the formation of more large-sized particles.[24] Therefore, the microwave heating temperature and time were set to be 120 °C and 30 min for the synthesis of these N-dots in further characterization and applications, respectively.

Characterization of N-dots

The size and morphology of N-dots formed with 2-azidoimidazole and glycerol under optimal microwave-assisted synthetic conditions were first characterized using a Transmission Electron Microscope (TEM). As shown in Fig. 1A, these N-dots exhibited quasi-spherical shapes with an average size of about 2.8 nm and a narrow size distribution (Fig. 1B). High-resolution TEM (HRTEM) clearly revealed a lattice spacing distance of 0.21 nm, which corresponded to the in-plane lattice spacing of graphite (100 facet).[25] The XRD pattern of N-dots showed that there was a broad peak at $2\theta = 23°$, which was consistent with the (002) lattice spacing of carbon-based materials with abundant sp^3 disorder (Fig. 1C).[26,27] The XRD result implied that these N-dots

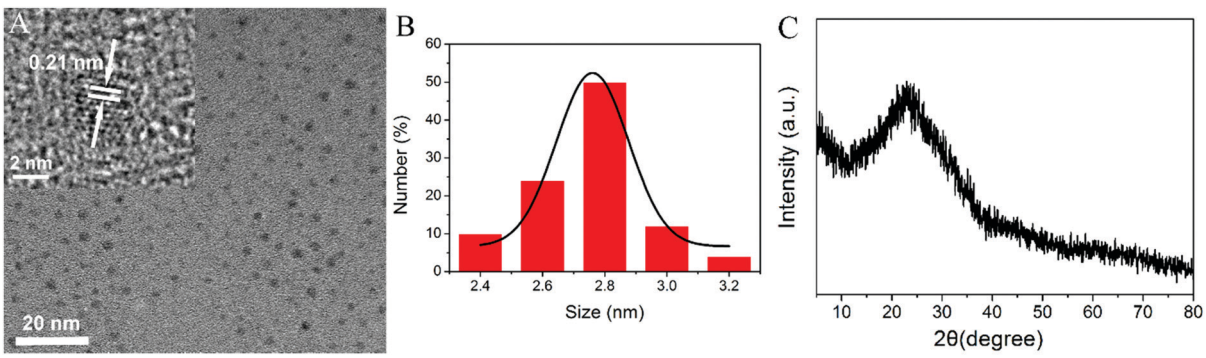

Fig. 1 The TEM and HRTEM (inset) images (A), the size distribution (B), and the powder XRD pattern (C) of the N-dots.

had an amorphous surface structure. In addition, the surface functional groups of the N-dots were characterized by FTIR. As shown in Fig. 2A, the stretching vibrations of –OH/–NH and C–H were located at 3400 cm^{-1} and 2940 cm^{-1}, respectively. The presence of the stretching vibration of C–NH–C at 1390 cm^{-1} confirmed the doping of nitrogen. In addition, the vibration peaks at 1630, 1110 and 1040 cm^{-1} could be ascribed to C═O vibration, C–O stretching and C–H bending, respectively.[28–31] The zeta potential of the N-dot aqueous solution was found to be −15.5 mV. The negative value of zeta potential was likely ascribed to the –COOH and –OH groups on the surface of the N-dots, which resulted in their excellent hydrophilicity and stability in an aqueous system.

XPS measurements were carried out to further explore the chemical composition and surface chemical components of the N-dots. In the high-resolution spectra, the C 1s spectrum (Fig. 2B) showed four peaks at 284.6, 285.2, 286.3, and 288.0 eV, which were attributed to C–C/C═C, C–N, C–O, and C═O/C═N functional groups, respectively.[32] The N 1s spectrum (Fig. 2C) contained three components that could be assigned to C–N═C (398.6 eV), N–$(C)_3$ (399.7 eV), and N–H (400.4 eV), respectively.[33] The two peaks at 531.3 and 532.4 eV in the O 1s spectrum (Fig. 2D) could be attributed to C═O and C–OH/C–O–C groups, respectively.[29] These results agreed well with those obtained from the FTIR measurements. In addition, the results from element content analysis of XPS revealed that the relative atomic percentages of C, N, and O in the obtained N-dot surface were 53.8%, 12.9%, and 22.7%, respectively. Combined with elemental analysis (35.3% for nitrogen element), a higher percentage of nitrogen element in the core of the N-dots was expected.

Optical properties of the N-dots

The UV-vis spectra of the N-dots (Fig. 3) showed an absorption peak at ∼219 nm, ascribed to the π–π* transition of the conjugated C═C units from the carbon core.[34] And a shoulder peak at ∼300 nm corresponded to n–π* transition of the C═O bond.[35] The N-dot aqueous solution was pale yellow, while it emitted intense cyan luminescence under irradiation using a 365 nm lamp (inset of Fig. 3). Unlike many other reported carbon dots,[36,37] the fluorescence emission of the N-dots was excitation-independent (Fig. 3). The excitation-independent fluorescence behavior of the prepared N-dots was ascribed to less surface defects and more uniform size,[25,38] which was consistent with TEM observation. The QY of the prepared N-dots was determined to be 27.9% using quinine sulfate as standard, which was higher than those of the surface-unmodified nitrogen-containing carbon dots in previous reports (typically <20%) and

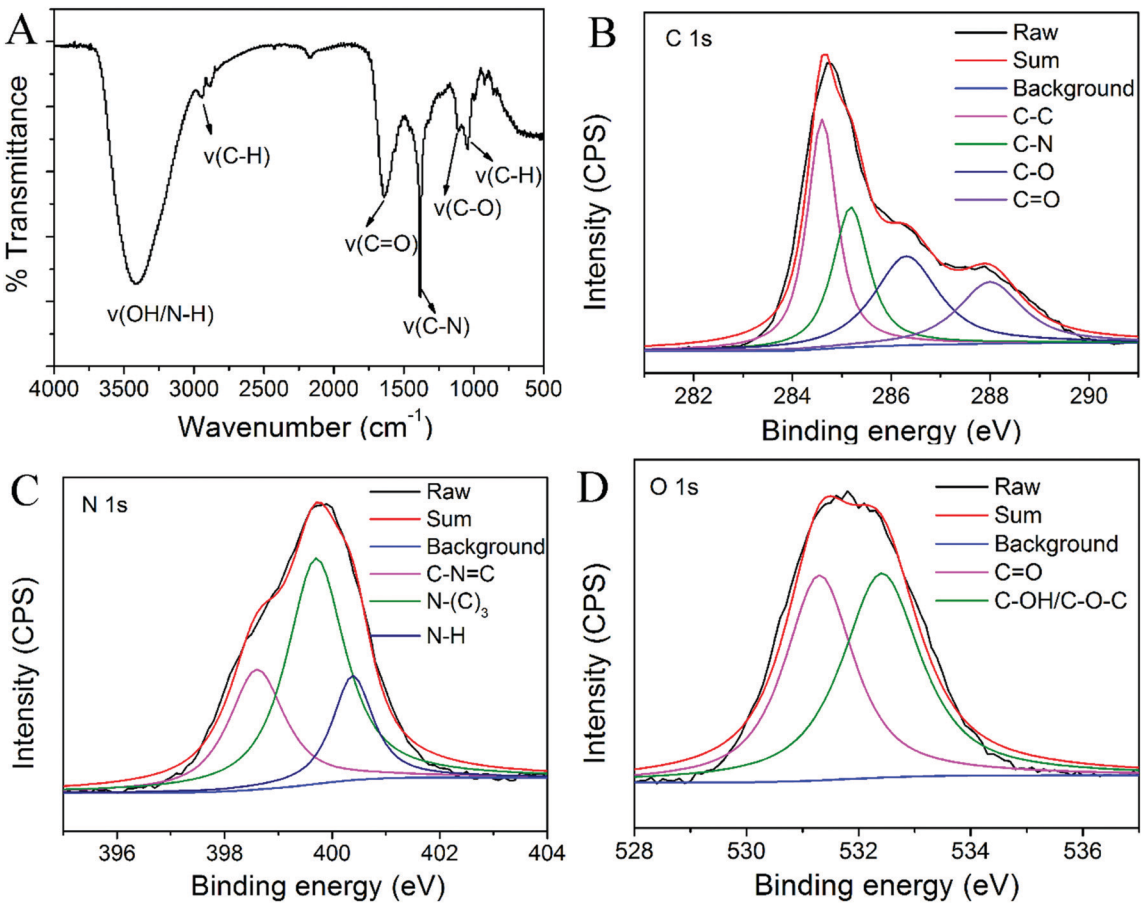

Fig. 2 (A) FT-IR spectrum of the N-dots. High resolution XPS spectra of (B) C 1s, (C) N 1s, and (D) O 1s peaks of the N-dots, respectively.

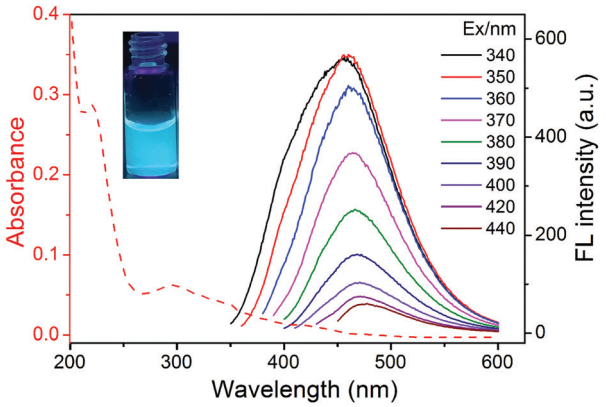

Fig. 3 UV-vis absorption and fluorescence emission spectra (with progressively longer excitation wavelengths from 340 to 480 nm) of the prepared N-dots. Inset shows a photograph of the N-dot aqueous solution under UV-light. (The concentration of the N-dot solution was 100 μg mL^{-1}.)

our previous report of N-dots with methanol (13%).[14,21,39,40] The higher QY may be ascribed to the chemical nature of the cross-linked internal core of the N-dots. The time-resolved fluorescence decay curve was also measured with a time-correlated single photon counting system. The decay curve was well fitted to a biexponential function and the mean lifetime of the N-dots was calculated to be 8.27 ns as illustrated in Fig. S5 and Table S5 (ESI†).

The stability of the N-dots under various conditions was further investigated. Fig. 4A and B demonstrated that the fluorescence intensities of the N-dots remained constant at relatively high ionic strengths (up to 200 mM NaCl) or under broad pH ranges (pH 3–11). In addition, there was no obvious attenuation in fluorescence intensity within 2 h of UV irradiation and it slightly decreased after 5 h continuous irradiation (Fig. 4C),

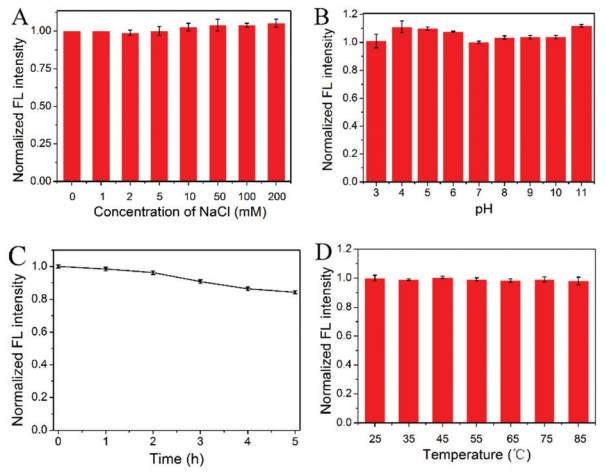

Fig. 4 (A) Normalized fluorescence intensity of the N-dots after addition of various concentrations of NaCl solutions. (B) Normalized fluorescence intensity of the N-dots at different pH values. (C) Normalized fluorescence intensity variation of the N-dots as a function of illumination time under 365 nm UV lamp (6 W). (D) Normalized fluorescence intensity of the N-dots after incubation at different temperatures for 10 min. Error bars were the standard deviation of three independent experiments. (The concentration of the N-dot solution was 100 μg mL^{-1}.)

suggesting that the N-dots were quite stable against light irradiation. When the incubation temperature of the N-dot solution increased from 25 to 85 °C, their fluorescence intensities remained almost unchanged, which indicated that these N-dots exhibited excellent thermostability (Fig. 4D). All of these features of N-dots promised great potential for future sensing applications.

Fluorescence sensing of Ag^+ using N-dots

As a representative heavy metal ion, silver has been widely employed in the photographic, medical and electronics industry.[41] It has brought serious environmental and health problems. Accumulation of silver in the human body causes many symptoms and diseases such as argyria and argyrosis, and other serious neurological, renal, or hepatic complications.[42,43] Thus the development of relatively cost-effective, selective and sensitive methods for determination of silver cations in environmental and biological systems is of important concern.

For the above N-dot solution, the addition of Ag^+ effectively quenched its fluorescence emission. The fluorescence quenching was quickly realized within 1 min. To explore the feasibility of using the N-dots for Ag^+ detection, the pH value of the detection solution was first optimized. As shown in Fig. S6 (ESI†), the Ag^+-induced fluorescence quenching efficiency reached its maximum in pH 7–8 PBS buffer solution of the N-dot solution. Under the optimized pH value of PBS buffer solution, the fluorescence intensity of the N-dot solution at 458 nm decreased gradually with the increase of Ag^+ concentration, and the fluorescence behavior could be clearly observed by the naked eye under a UV lamp, as shown in Fig. 5A. The quenching efficiency (F_0/F, where F_0 and F were the fluorescence intensities in the absence and presence of the Ag^+, respectively) was in a distinct linear relationship with the concentration of Ag^+ in the range from 20 nM to 6 μM, with R^2 of 0.997 (Fig. 5B). The limit of detection (LOD) was then calculated to be 6.3 nM ($3s/k$, in which s was the standard deviation for the control and k was the slope of the calibration curve), which was much lower than the toxicity level of Ag^+ cations in drinking water (460 nM) defined by the U.S. Environmental Protection Agency (EPA).[44] Moreover, the LOD value was comparable with or even lower than those obtained from other methods reported for Ag^+ sensing[15,45–51] (Table S6, ESI†). These data indicated that the N-dots could achieve satisfactory sensitivity for Ag^+ detection.

To estimate the selectivity of N-dots for the detection of Ag^+, the fluorescence changes in the presence of representative interferents were then investigated. As shown in Fig. 5C, most common metallic ions including Na^+, K^+, Mg^{2+}, Ca^{2+}, Co^{2+}, Cd^{2+}, Fe^{2+}, Fe^{3+}, and Cr^{3+} exhibited a negligible effect on the fluorescence intensity at 458 nm even at a concentration 40-fold higher than that of the Ag^+ cations. It was worth noting that Cu^{2+} and Hg^{2+} could lead to a slight fluorescence decrease of the N-dot solution when their concentrations reached up to 5 μM. It is well known that EDTA could form stable complexes with Hg^{2+} and Cu^{2+}, and it had little effect on Ag^+.[52] To eliminate the interference of Hg^{2+} and Cu^{2+} on the fluorescence of the N-dots, EDTA was chosen as a masking agent. As indicated in Fig. S7 (ESI†), both Hg^{2+} and Cu^{2+} did not induce an obvious change in

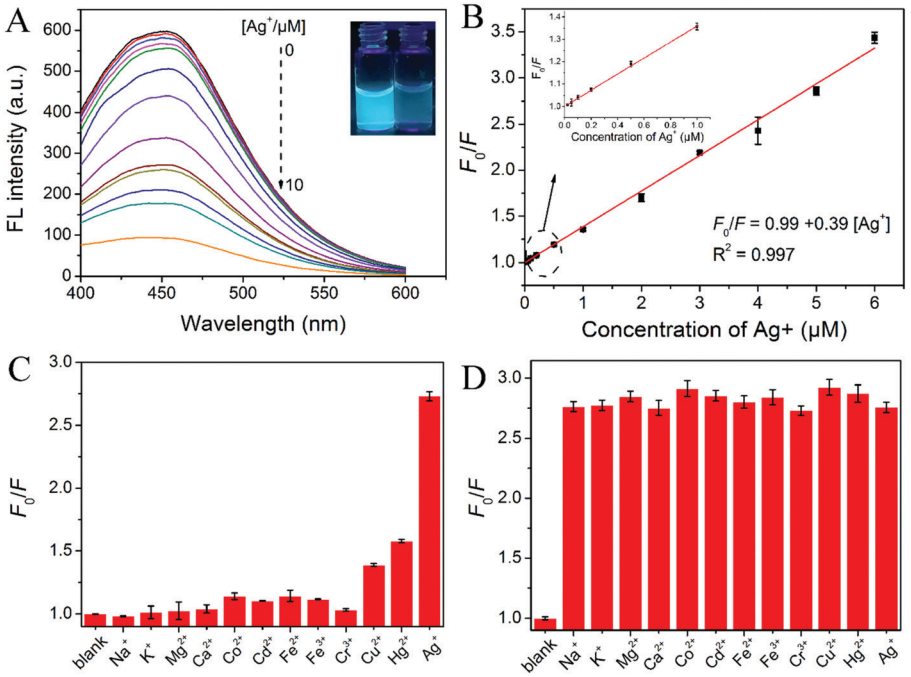

Fig. 5 (A) The fluorescence emission spectra of the N-dots in the presence of various concentrations of Ag^+ in PBS (10 mM, pH 7.4) buffer solution (the Ag^+ concentration from top to down was: 0, 0.02, 0.05, 0.1, 0.2, 0.5, 1, 2, 3, 4, 5, 6, and 10 μM). Inset shows photographs of the N-dot solution in the absence and presence of 6 μM Ag^+ under UV light (365 nm). (B) The linear relationship between the fluorescence quenching efficiency (F_0/F) variation and the Ag^+ concentration in the range from 20 nM to 6 μM. (C) Selectivity of the nanoprobe for Ag^+ over other representative metal ions (5 μM for Cu^{2+}, Hg^{2+} and Ag^+. 200 μM for other cations). (D) Fluorescence response of the nanoprobe against 5 μM Ag^+ with the coexistence of other ions (20 μM for Cu^{2+} and Hg^{2+}. 200 μM for other cations). Error bars were the standard deviation of three independent experiments. (The concentration of the N-dot solution was 100 μg mL^{-1}.)

the fluorescence intensity of the N-dots any more after the addition of EDTA. Moreover, the anti-interference performance of the Ag^+ sensing system was also evaluated. As presented in Fig. 5D, the fluorescence responses of the N-dot solution to Ag^+ were almost unchanged after the addition of relatively high concentrations of other interferents to the sensing system. Based on the above results, the N-dot probe exhibited an excellent selectivity and strong tolerance toward Ag^+ sensing, which might be directly applied in real samples.

To investigate the quenching mechanism of the N-dots for Ag^+ sensing, further experiments were performed. Generally, the fluorescence could be quenched by the dynamic quenching effect (DQE) or static quenching effect (SQE) or both simultaneously. For N-dots, the relationship between the fluorescence quenching efficiency and the concentration of Ag^+ was well fitted to the Stern–Volmer equation ($F_0/F = 1 + K_{SV}[Q]$, where F_0 and F were the fluorescence intensities in the absence and presence of the quencher, respectively; Q was the concentration of the quencher), which indicated that there was only one quenching mechanism (DQE or SQE) in this system.[53] To further gain insight into the fluorescence quenching mechanism, the fluorescence decay curves of the N-dots in the absence and presence of Ag^+ were also investigated. As shown in Fig. 6A and Table S5 (ESI†), there were almost no changes in the lifetime for the N-dots before and after the addition of Ag^+. These data suggested that the above fluorescence quenching could be mainly due to SQE, rather than DQE.[54,55] To confirm the SQE quenching mechanism during the

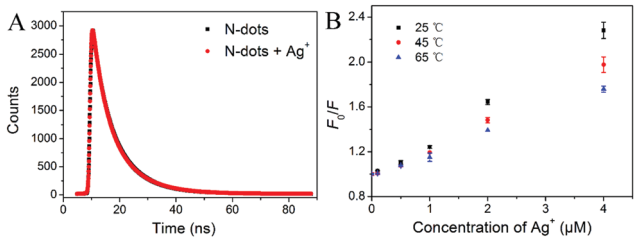

Fig. 6 (A) Time-resolved fluorescence decay curves of the N-dot solution before and after the addition of 10 μM Ag^+. (B) Stern–Volmer plots at three different temperatures. (The concentration of the N-dot solution was 100 μg mL^{-1}.)

Ag^+ sensing process, the quenching constants at three different temperatures (25, 45, 65 °C) were investigated. As shown in Fig. 6B, the quenching constant was inversely correlated with the temperature. Along with the phenomenon that the UV-vis absorption spectrum of the N-dots changed after the addition of Ag^+ (Fig. S8, ESI†), it was confirmed that the quenching mechanism of the N-dots/Ag+ system was initiated by complex formation of Ag^+ and N-dots rather than dynamic collision.[56,57]

Applications of N-dots as a fluorescence sensor

To evaluate the practicality of the proposed fluorescence organic quantum dot sensor, Ag^+ detection was carried out in real samples such as tap water and human urine. Samples spiked with three different concentrations (0.1 μM, 0.5 μM and 2 μM) of

Ag^+ were studied. The recovery tests of each concentration were carried out in triplicate and the averages were presented with standard deviation. As shown in Table 1, the concentrations of Ag^+ found were close to the spiked values by the proposed method and the recoveries ranged from 92.5% to 110.3% at three different concentrations of Ag^+. The above results indicated the utility and reliability of the fluorescence probe for detection of Ag^+.

As Ag^+ has a high affinity preference to biothiols as a thiophilic metal ion, Ag^+ could be competitively captured by biothiols from the N-dots/Ag^+ complex. As shown in Fig. S9 and S10 (ESI†), with the addition of common amino acids to the N-dots/Ag^+ complex, only biothiols such as cysteine (Cys), homocysteine (Hcy) and glutathione (GSH) led to obvious fluorescence recovery. Therefore, a ''turn-on'' fluorescence probe for biothiol detection could be implemented based on the N-dots/Ag^+ complex in future.

Experimental

Reagents and chemicals

Propanol and 1,2-propanediol were purchased from Sinopharm Chemical Reagent Co., Ltd (Shanghai, China). Glycerol was purchased from Beijing Biotopped Science & Technology Co., Ltd (Beijing, China). 2-Azidoimidazole was synthesized according to the previous method.[14] All reagents were of analytical reagent grade and used without further purification, and doubly distilled water was used throughout.

Synthesis of N-dots

N-Dots were prepared by a facile microwave-assisted heating method which used 2-azidoimidazole and hydroxyl compounds (propanol, 1,2-propanediol, and glycerol) as the carbon sources. Typically, 2-azidoimidazole, hydroxyl compounds and ultrapure water were mixed homogeneously. The transparent solution was transferred into a microwave synthesizer and heated under 120 °C, 150 psi and 50 W for 30 min. In the process of microwave heating, the solution colour changed from transparent to brown as a result of formation of N-dots. After cooling to room temperature, the solution was centrifuged at 6000 rpm to remove large particles. Finally, the N-dots were purified by dialyzing against deionized water through a dialysis membrane (300–500 Da) for 24 h and then freeze-dried for further characterization and fluorescence measurements.

Table 1 Results of determination of Ag^+ cation in tap water and human urine samples by the proposed method

Sample	Added (μM)	Found[a] (μM)	Recovery (%)
Tap water	0.1	0.098 ± 0.017	98.3
	0.5	0.54 ± 0.033	108.8
	2	2.00 ± 0.049	100.3
Urine	0.1	0.11 ± 0.020	110.3
	0.5	0.52 ± 0.025	104.4
	2	1.96 ± 0.041	97.9

[a] Value = mean ± SD (n = 3).

Characterization of N-dots

The microwave synthesis of N-dots was performed on a Discover SP microwave synthesizer (CEM, USA). Transmission electron microscopic (TEM) images were acquired on a JEM-2100F microscope (JEOL, Japan). Fourier transform infrared spectroscopic (FTIR) spectra were collected on a Nexus 470 spectrometer (Thermo Nicolet, USA). X-ray photoelectron spectroscopic (XPS) measurements were carried out on an ESCALAB 250Xi spectrometer (Thermo, USA). Fluorescence lifetimes were measured using an FLS1000 time-corrected-single-photon-counting system. Zeta potential was measured on a Malvern Zetasizer Nano ZS (Malvern, UK). UV-vis absorption spectra were recorded using a DU 800 UV-vis spectrophotometer (Beckman, USA). Fluorescence emission spectra were measured on a Cary Eclipse fluoro spectrophotometer (Agilent, USA).

Quantum yield (QY) measurements

Quinine sulphate in 0.1 M H_2SO_4 (QY = 0.54 at 350 nm) was chosen as a standard. The QY of the N-dots in water was calculated according to the following equation:

$$Q = Q_r \times \frac{A_r}{A} \times \frac{I}{I_r} \times \frac{n^2}{n_r^2}$$

where Q is quantum yield; I is the measured integrated fluorescence emission intensity; A is the absorbance measured at the excitation wavelength; n is the refractive index (1.33 for water). The subscript ''r'' designates the reference fluorophore of known quantum yield. In order to minimize reabsorption effects, the absorbance value of the individual solution was kept below 0.05 at the excitation wavelength of 350 nm.

Fluorescence detection of Ag^+

10 μL of the prepared N-dot stock solution (10 mg mL^{-1}) was mixed with 980 μL sodium phosphate buffer (PBS, 10 mM, pH 7.4). Then 10 μL of $AgNO_3$ standard solution with different concentrations was added and vortex-mixed for 1 min at room temperature. Their fluorescence emission spectra were then recorded at an excitation wavelength of 350 nm.

To investigate the selectivity of N-dots on Ag^+ sensing, its fluorescence responses to other metallic ions (200 μM for Na^+, K^+, Mg^{2+}, Ca^{2+}, Co^{2+}, Cd^{2+}, Fe^{2+}, Fe^{3+}, and Cr^{3+}. 5 μM for Cu^{2+}, Hg^{2+}) were examined following the same procedure to that of Ag^+ mentioned above. For the interference study of other metal ions, metallic ions with certain concentrations (200 μM for Na^+, K^+, Mg^{2+}, Ca^{2+}, Co^{2+}, Cd^{2+}, Fe^{2+}, Fe^{3+}, and Cr^{3+}. 20 μM for Cu^{2+}, Hg^{2+}) were mixed with the probe in the PBS buffer, respectively, and the fluorescence intensities of the N-dot solutions at 458 nm were measured by a fluorescence spectrophotometer. Then, 5 μM of Ag^+ ion was further introduced to the probe solution and the fluorescence emission intensities at 458 nm were collected, respectively.

Fluorescence quenching mechanism of Ag^+/N-dots

In order to investigate the quenching constants at different temperatures, 10 μL of $AgNO_3$ standard solution with different

concentrations was added to 1 mL of N-dot solution (100 μg mL^{-1} in PBS buffer, pH 7.4) at 25, 45 and 65 °C, respectively. The fluorescence emission spectra were then recorded at an excitation wavelength of 350 nm.

To investigate the change of fluorescence lifetimes in the N-dots with the addition of Ag^+, the time-resolved fluorescence decay curves of the N-dot solutions (100 μg mL^{-1}) were measured in the absence and presence of Ag^+ (10 μM), respectively.

Detection of Ag^+ cation in real samples

The tap water sample was collected from our lab and filtered using a 0.45 μm filter to remove possible solid suspensions. The human urine was obtained from a healthy volunteer and subjected to 50-fold dilution for subsequent analysis. A volume of 10 μL of diluted samples with different concentrations of Ag^+ were added to the sensing system, and the resultant fluorescence spectra were recorded.

Fluorescence detection of biothiols using N-dots/Ag^+ complexes

For the detection of biothiols, the N-dot solution (100 μg mL^{-1} in PBS buffer, pH 7.4) was first mixed with Ag^+ (6 μM). Then, various concentrations of biothiols such as cysteine (Cys), homocysteine (Hcy) and glutathione (GSH) were added. After 5 min, the fluorescence spectra of the mixture solutions were recorded.

To evaluate the selectivity of the N-dots/Ag^+ complex solution for biothiols, interferents were added instead of biothiols under the same experimental conditions. All the fluorescence spectra were recorded under excitation at 350 nm, and the emission intensities at 458 nm were recorded.

Conclusions

In summary, we described a facile approach to the synthesis of highly fluorescent N-dots using 2-azidoimidazole and hydroxyl compounds with different numbers of hydroxyl groups as crosslink additives. Employment of a microwave heating strategy and the assistance of appropriate crosslinking additives effectively improved the fluorescence emission efficiency of the N-dots, yielding a QY up to 27.9% with glycerol as the additive. The N-dots exhibited uniform size distribution, excellent water-solubility, and good stability against pH, temperature, ionic strength as well as light illumination, and could serve as a fluorescence probe for Ag^+ sensing. The Ag^+-mediated fluorescence quenching was attributed to the static quenching effect after the chelation of Ag^+ and N-dots. This sensing system showed high sensitivity, good selectivity toward Ag^+ and low detection limit, and thus it could be a promising candidate for monitoring the Ag^+ in real systems.

Conflicts of interest

There are no conflicts to declare.

Acknowledgements

This work was supported by the National Natural Science Foundation of China (Grants No. 21672015 and 21708001), the National Major Scientific and Technological Special Project for "Significant New Drugs Development" (Grant No. 2017ZX09303013) and the China Postdoctoral Science Foundation (Grant No. 2018M631272).

Notes and references

1 J. Du, N. Xu, J. Fan, W. Sun and X. Peng, *Small*, 2019, **15**, 1805087.
2 M. Li, T. Chen, J. J. Gooding and J. Liu, *ACS Sens.*, 2019, **4**, 1732–1748.
3 B. Wang, J. Li, Z. Tang, B. Yang and S. Lu, *Sci. Bull.*, 2019, **64**, 1285–1292.
4 M. Pirsaheb, A. Asadi, M. Sillanpää and N. Farhadian, *J. Mol. Liq.*, 2018, **271**, 857–871.
5 Y. Liu, Y. Yang, Z. Peng, Z. Liu, Z. Chen, L. Shang, S. Lu and T. Zhang, *Nano Energy*, 2019, **65**, 104023.
6 F. Wang, Y. H. Chen, C. Y. Liu and D. G. Ma, *Chem. Commun.*, 2011, **47**, 3502–3504.
7 S. Lu, L. Sui, J. Liu, S. Zhu, A. Chen, M. Jin and B. Yang, *Adv. Mater.*, 2017, **29**, 1603443.
8 X. Yan, X. Cui, B. Li and L. S. Li, *Nano Lett.*, 2010, **10**, 1869–1873.
9 Y. F. Kang, Y. W. Fang, Y. H. Li, W. Li and X. B. Yin, *Chem. Commun.*, 2015, **51**, 16956–16959.
10 J. Wang, C. F. Wang and S. Chen, *Angew. Chem., Int. Ed.*, 2012, **51**, 9297–9301.
11 K. Jiang, S. Sun, L. Zhang, Y. Lu, A. Wu, C. Cai and H. Lin, *Angew. Chem., Int. Ed.*, 2015, **54**, 5360–5363.
12 G. Zuo, A. Xie, J. Li, T. Su, X. Pan and W. Dong, *J. Phys. Chem. C*, 2017, **121**, 26558–26565.
13 G. Zuo, A. Xie, X. Pan, T. Su, J. Li and W. Dong, *ACS Appl. Nano Mater.*, 2018, **1**, 2376–2385.
14 X. Chen, Q. Jin, L. Wu, C. Tung and X. Tang, *Angew. Chem., Int. Ed.*, 2014, **53**, 12542–12547.
15 Z. Wu, M. Feng, X. Chen and X. Tang, *J. Mater. Chem. B*, 2016, **4**, 2086–2089.
16 B. J. Yoon, E. H. Hong, S. E. Jee, D. M. Yoon, D. S. Shim, G. Y. Son, Y. J. Lee, K. H. Lee, H. S. Kim and C. G. Park, *J. Am. Chem. Soc.*, 2005, **127**, 8234–8235.
17 Y. Takagi, L. Tauchi, H. D. Nguyen-Tran, T. Ohta, M. Shimizu and K. Ohta, *J. Mater. Chem.*, 2011, **21**, 14569–14574.
18 H. Nie, M. Cui and T. P. Russell, *Chem. Commun.*, 2013, **49**, 5159–5161.
19 A. M. Schwenke, S. Hoeppener and U. S. Schubert, *Adv. Mater.*, 2015, **27**, 4113–4141.
20 L. Tang, R. Ji, X. Cao, J. Lin, H. Jiang, X. Li, K. S. Teng, C. M. Luk, S. Zeng, J. Hao and S. P. Lau, *ACS Nano*, 2012, **6**, 5102–5110.
21 C. Liu, P. Zhang, X. Zhai, F. Tian, W. Li, J. Yang, Y. Liu, H. Wang, W. Wang and W. Liu, *Biomaterials*, 2012, **33**, 3604–3613.
22 S. Zhu, Y. Song, J. Shao, X. Zhao and B. Yang, *Angew. Chem., Int. Ed.*, 2015, **54**, 14626–14637.
23 S. Tao, Y. Song, S. Zhu, J. Shao and B. Yang, *Polymer*, 2017, **116**, 472–478.

24 Q. Wang, H. Zheng, Y. Long, L. Zhang, M. Gao and W. Bai, *Carbon*, 2011, **49**, 3134–3140.
25 Y. Dong, H. Pang, H. B. Yang, C. Guo, J. Shao, Y. Chi, C. M. Li and T. Yu, *Angew. Chem., Int. Ed.*, 2013, **52**, 7800–7804.
26 V. Ramanan, S. K. Thiyagarajan, K. Raji, R. Suresh, R. Sekar and P. Ramamurthy, *ACS Sustainable Chem. Eng.*, 2016, **4**, 4724–4731.
27 Y. Zhong, J. Li, Y. Jiao, G. Zuo, X. Pan, T. Su and W. Dong, *J. Lumin.*, 2017, **190**, 188–193.
28 B. Kong, A. Zhu, C. Ding, X. Zhao, B. Li and Y. Tian, *Adv. Mater.*, 2012, **24**, 5844–5848.
29 L. Lin, M. Rong, S. Lu, X. Song, Y. Zhong, J. Yan, Y. Wang and X. Chen, *Nanoscale*, 2015, **7**, 1872–1878.
30 F. Arcudi, L. Đorđević and M. Prato, *Angew. Chem., Int. Ed.*, 2016, **55**, 2107–2112.
31 J. Li, G. Zuo, X. Pan, W. Wei, X. Qi, T. Su and W. Dong, *Luminescence*, 2018, **33**, 243–248.
32 S. Liu, J. Tian, L. Wang, Y. Zhang, X. Qin, Y. Luo, A. M. Asiri, A. O. Al-Youbi and X. Sun, *Adv. Mater.*, 2012, **24**, 2037–2041.
33 S. Liu, J. Tian, L. Wang, Y. Luo, J. Zhai and X. Sun, *J. Mater. Chem.*, 2011, **21**, 11726–11729.
34 P. Roy, P. C. Chen, A. P. Periasamy, Y. N. Chen and H. T. Chang, *Mater. Today*, 2015, **18**, 447–458.
35 Z. Luo, Y. Lu, L. A. Somers and A. T. C. Johnson, *J. Am. Chem. Soc.*, 2009, **131**, 898–899.
36 Y. Zhang, X. Liu, Y. Fan, X. Guo, L. Zhou, Y. Lv and J. Lin, *Nanoscale*, 2016, **8**, 15281–15287.
37 C. Wang, Z. Xu, H. Cheng, H. Lin, M. G. Humphrey and C. Zhang, *Carbon*, 2015, **82**, 87–95.
38 Z. Yang, M. Xu, Y. Liu, F. He, F. Gao, Y. Su, H. Wei and Y. Zhang, *Nanoscale*, 2014, **6**, 1890–1895.
39 X. Jia, J. Li and E. Wang, *Nanoscale*, 2012, **4**, 5572–5575.
40 Z. Zhang, J. Hao, J. Zhang, B. Zhang and J. Tang, *RSC Adv.*, 2012, **2**, 8599–8601.
41 Y. Wen, F. Xing, S. He, S. Song, L. Wang, Y. Long, D. Li and C. Fan, *Chem. Commun.*, 2010, **46**, 2596–2598.
42 S. S. Tan, Y. N. Teo and E. T. Kool, *Org. Lett.*, 2010, **12**, 4820–4823.
43 Z. Lin, X. Li and H.-B. Kraatz, *Anal. Chem.*, 2011, **83**, 6896–6901.
44 H. T. Ratte, *Environ. Toxicol. Chem.*, 1999, **18**, 89–108.
45 V. Borse, M. Thakur, S. Sengupta and R. Srivastava, *Sens. Actuators, B*, 2017, **248**, 481–492.
46 Y. Jiao, Y. Gao, Y. Meng, W. Lu, Y. Liu, H. Han, S. Shuang, L. Li and C. Dong, *ACS Appl. Mater. Interfaces*, 2019, **11**, 16822–16829.
47 K. Jiang, S. Sun, L. Zhang, Y. Wang, C. Cai and H. Lin, *ACS Appl. Mater. Interfaces*, 2015, **7**, 23231–23238.
48 Y. Chang, Z. Zhang, J. Hao, W. Yang and J. Tang, *Sens. Actuators, B*, 2016, **232**, 692–697.
49 C. Wu, C. Xiong, L. Wang, C. Lan and L. Ling, *Analyst*, 2010, **135**, 2682–2687.
50 X. Li, Z. Wu, X. Zhou and J. Hu, *Biosens. Bioelectron.*, 2017, **92**, 496–501.
51 S. Bian, C. Shen, Y. Qian, J. Liu, F. Xi and X. Dong, *Sens. Actuators, B*, 2017, **242**, 231–237.
52 T. Lou, Z. Chen, Y. Wang and L. Chen, *ACS Appl. Mater. Interfaces*, 2011, **3**, 1568–1573.
53 S. Soares, N. Mateus and V. de Freitas, *J. Agric. Food Chem.*, 2007, **55**, 6726–6735.
54 J. R. Lakowicz, *Principles of fluorescence spectroscopy*, Springer Science & Business Media, 2013.
55 C. Zhou, X. He, D. Ya, J. Zhong and B. Deng, *Sens. Actuators, B*, 2017, **249**, 256–264.
56 Y. J. Hu, Y. Liu, Z. B. Pi and S. S. Qu, *Bioorg. Med. Chem.*, 2005, **13**, 6609–6614.
57 Y. Z. Zhang, X. X. Chen, J. Dai, X. P. Zhang, Y. X. Liu and Y. Liu, *Luminescence*, 2008, **23**, 150–156.

